PERGAMON

Automatica 36 (2000) 427–438

www.elsevier.com/locate/automatica

Brief Paper

Guidance and control of a launch vehicle using a stochastic gradient projection method☆

Fernando Madeira[a,*], Atair Rios-Neto[b]

[a]*Flight Mechanics Group, Section of Aerodynamics and Aeroelasticity, EMBRAER, São José dos Campos, 12227-901, SP, Brazil*
[b]*Institute of Research and Development, University of Paraiba Valley, UNIVAP, São José dos Campos, 12245-720, SP, Brazil*

Received 10 December 1997; revised 21 April 1999; received in final form 7 June 1999

Abstract

A recently developed nonlinear programming stochastic projection of the gradient-type technique is applied to get and test novel procedures for tri-dimensional guidance and control of a satellite solid-fuel launch vehicle. Near optimal open-loop and low-frequency closed-loop solutions are obtained by parametrization of the control history and by considering the satisfaction of boundary constraints unless of specified random errors. Numerical simulations and tests show that the closed-loop solution can cope with the typical model uncertainties and environmental perturbations. A non standard situation of having a fourth stage with a free burning time is tested.

Keywords: Satellite launch vehicle; Stochastic gradient projection; Trajectory optimization

1. Introduction

Orbital injection usually requires the application of an optimal guidance and control procedure in order to maximize payload and accurately place it into the desired orbit without violating mission constraints. The high costs involved in satellite launching fully justify the high research efforts and budgets in order to improve solution methods in terms of optimization, ease of use and robustness to environmental perturbations and modeling errors.

Guidance and control procedures may be applied in both an open or closed-loop fashion. Open-loop guidance and control procedures apply a control history found off-line prior to the flight. Works on this subject determine the control history usually by solving a trajectory optimization problem (Breakwell, 1959). A wide variety of methods have been devised recently and applied to different purposes (Lu, 1993; Hargraves & Paris, 1987; Betts & Huffman, 1991; Enright & Conway, 1992; Burlirsch & Chudej, 1992; Betts, 1994; Tang & Conway, 1995; Seywald, 1993; Coverstone-Carroll & Williams, 1994; Sachs, Drexler & Stich (1991); Smania & Rios Neto 1988).

Closed-loop guidance and control procedures are conceived to cope with uncertainties and perturbations ever present during the flight. Great efforts have been devoted to devising guidance and control procedures, fast enough and reliable enough to be applied onboard the flying vehicle. Research works include a broad range of approaches in which their complexities are strongly dependent on the current onboard computer technology. The majority consists of a trajectory optimization procedure further simplified to meet the real time feasibility. Recent works on this subject include the utilization of explicit guidance (Sinha, Shrivastava, Bhat & Prabhu, 1989; Vittal & Bhat, 1991), energy state methods (Corban, Calise & Flandro, 1991), dynamic programming (Feeley & Speyer, 1994), generalized projected gradient (Richard & Christophe, 1995), finite element (Hodges, Calise, Bless & Leung, 1992; Leung & Calise, 1994), hybrid analytic/numerical approach (Leung & Calise, 1994), neighboring extremals (da Silva, 1994), geometrical approach (Mease & van Buren, 1994), etc. Another emergent approach consists of application of parallel processing techniques to speedup the overall trajectory

☆This paper was not presented at any IFAC meeting. This paper was recommended for publication in revised form by Associate Editor J. Sasiadek under the direction of Editor K. Furuta.

* Corresponding author. Tel.: + 55-12-345-1457; fax: + 55-12-345-1723.

E-mail address: fmadeira@embraer.com.br (F. Madeira)

0005-1098/00/$ - see front matter
PII: S0005-1098(99)00163-6

optimization computation time (Betts & Huffman, 1991; Psiaki & Park, 1992; Wirthman, Park & Vadali, 1995).

This paper presents the first application of a recently developed stochastic gradient projection method to optimal design and closed-loop guidance and control of a launch vehicle trajectory. The version of the stochastic gradient projection method used was proposed by Rios Neto and Pinto (1987). The success of its application in solving problems of spacecraft maneuvers (Prado & Rios Neto, 1994; Rios Neto & Madeira, 1997) motivated its application in guidance and control of launch vehicle. A direct search method using this nonlinear programming technique is implemented. The trajectory is divided into a sequence of segments and the control history is approximated by parametrized functions inside each trajectory segment. The objective is to find a parametrized control history to place the maximum satellite mass in a low Earth orbit. A low frequency closed-loop guidance and control procedure intended for onboard use is formulated and tested.

A special feature of this method is the inclusion of the acceptable errors on the constraints into the problem resolution. Therefore, instead of searching a solution that corresponds to a definite value for every constraint component, the method searches solutions that make each constraint component to fall inside a given interval.

Simulations and tests are carried out for the satellite launch vehicle (VLS) of the Brazilian Complete Space Mission (MEC-B).

The following sections present a brief review underlying the major features of the stochastic gradient projection method, the launch vehicle open-loop trajectory optimization, and the closed-loop guidance and control procedure.

2. Stochastic gradient projection method: a review

2.1. Statement of the problem

Consider the nonlinear programming problem stated as

$$\text{Minimize} \quad F(\mathbf{Y}) \tag{1}$$

$$\text{subject to} \quad \mathbf{h}(\mathbf{Y}) = \boldsymbol{\varepsilon}, \quad \mathbf{g}(\mathbf{Y}) \le \boldsymbol{\delta}, \tag{2}$$

in which $\mathbf{Y}$ is a n-dimensional vector of parameters to be optimized; F, $\mathbf{h}$, and $\mathbf{g}$ are real-valued functions of $\mathbf{Y}$ of dimensions 1, m_h, and m_g, respectively; $\boldsymbol{\varepsilon}$ and $\boldsymbol{\delta}$ the error vectors, representing the acceptable accuracy on the constraints satisfaction, defined as

$$|\varepsilon_i| \le \varepsilon_i^t, \quad i = 1,2,\ldots,m_h,$$

$$|\delta_j| \le \delta_j^t, \quad j = 1,2,\ldots,m_g, \tag{3}$$

where ε_i^t and δ_j^t are given and fixed accuracy limits of constraints satisfaction, defining the region within which the errors are considered tolerable, and which can be viewed as modeling the numerical zero for each constraint satisfaction.

2.2. Solution of the problem

In a typical iteration, one searches an approximate solution for the first-order increment $\Delta\mathbf{Y}$ in the problem:

$$\text{Minimize} \quad F(\bar{\mathbf{Y}} + \Delta\mathbf{Y}) \tag{4}$$

$$\text{subject to} \quad \mathbf{h}(\bar{\mathbf{Y}} + \Delta\mathbf{Y}) = \alpha\mathbf{h}(\bar{\mathbf{Y}}) + \boldsymbol{\varepsilon},$$

$$g_i(\bar{\mathbf{Y}} + \Delta\mathbf{Y}) = \beta g_i(\bar{\mathbf{Y}}) + \delta_i, \tag{5}$$

in which $\bar{\mathbf{Y}}$ is a given initial guess or a point from the last iteration; $g_i(\bar{\mathbf{Y}}) \ge \delta_i^t$, $i = 1,2,\ldots,I_g$, represent the set of active constraints; $0 \le \alpha < 1$ and $0 \le \beta < 1$ are the search step adjustment parameters chosen in order to condition $\Delta\mathbf{Y}$ to be of first order of magnitude, i.e., for a highly nonlinear constraint, the associated search step parameter value should be closer to the unity; on the other hand, for a fairly linear constraint, the associated search step value may be selected closer to zero.

The left-hand sides of Eqs. (5) are replaced by linearized approximations together with a stochastic interpretation for the errors $\boldsymbol{\varepsilon}$ and δ_i, leading to

$$(\alpha - 1)\mathbf{h}(\bar{\mathbf{Y}}) = \frac{\mathrm{d}\mathbf{h}(\bar{\mathbf{Y}})}{\mathrm{d}\mathbf{Y}}\Delta\mathbf{Y} + \boldsymbol{\varepsilon}^{\mathrm{r}},$$

$$(\beta - 1)g_i(\bar{\mathbf{Y}}) = \frac{\mathrm{d}g_i}{\mathrm{d}\mathbf{X}}\Delta\mathbf{Y} + \delta_i^{\mathrm{r}}. \tag{6}$$

In Eqs. (6), the error vectors were converted into the uniformly distributed unbiased noncorrelated random errors $\boldsymbol{\varepsilon}^{\mathrm{r}}$ and δ_i^{r}, modeled as

$$E[\boldsymbol{\varepsilon}^{\mathrm{r}}\boldsymbol{\varepsilon}^{\mathrm{r}^{\mathrm{T}}}] = diag[e_i^2,\ i = 1,2,\ldots,m_h], \qquad e_i^2 = \tfrac{1}{3}(\varepsilon_i^t)^2,$$

$$E[\boldsymbol{\delta}^{\mathrm{r}}\boldsymbol{\delta}^{\mathrm{r}^{\mathrm{T}}}] = diag[d_i^2,\ i = 1,2,\ldots,I_g], \qquad d_j^2 = \tfrac{1}{3}(\delta_j^t)^2. \tag{7}$$

The condition stated by (4) is approximated by the following a priori information:

$$-\gamma\nabla F^{\mathrm{T}}(\bar{\mathbf{Y}}) = \Delta\mathbf{Y} + \boldsymbol{\eta}, \tag{8}$$

in which γ is a nonnegative search step to be adjusted such that the increment $\Delta\mathbf{Y}$ turns out to be of first order of magnitude; $\boldsymbol{\eta}$ is a uniformly distributed unbiased random vector modeling the a priori searching error in the negative direction of the gradient $\nabla F(\bar{\mathbf{Y}})$, given by

$$E[\boldsymbol{\eta}\boldsymbol{\eta}^{\mathrm{T}}] = \bar{\mathbf{P}}, \tag{9}$$

where $\bar{\mathbf{P}}$ is taken to be diagonal, since no a priori correlation is imposed among the errors in the gradient components, and with variances adjusted by maximum likelihood statistical criteria such as to have the η dispersion to be of first order of magnitude as compared to the second order of magnitude of errors ε^r and δ_i^r.

The nonlinear programming problem given by Eqs. (1) and (2) has been converted into the linearized problem of Eqs. (8) and (6). The linearized problem, in turn, characterizes a parameter linear estimation problem:

$$\Delta\bar{\mathbf{Y}} = \Delta\mathbf{Y} + \boldsymbol{\eta},$$

$$\mathbf{Z} = \mathbf{M}\Delta\mathbf{Y} + \mathbf{V}, \tag{10}$$

in which Eq. (10) is equivalent respectively to Eqs. (8) and (6), using a shorthand notation.

Adopting a criterion of linear, minimum variance estimation, the optimal search increment can be determined using the Gauss–Markov–Kalman estimator (Jazwinski, 1970).

$$\Delta\hat{\mathbf{Y}} = \Delta\bar{\mathbf{Y}} + \mathbf{K}(\mathbf{Y} - \mathbf{M}\Delta\bar{\mathbf{Y}}),$$

$$\mathbf{P} = \bar{\mathbf{P}} - \mathbf{K}\mathbf{M}\bar{\mathbf{P}},$$

$$\mathbf{K} = \bar{\mathbf{P}}\mathbf{M}^{\mathrm{T}}(\mathbf{M}\bar{\mathbf{P}}\mathbf{M}^{\mathrm{T}} + \mathbf{R})^{-1}, \tag{11}$$

in which $\mathbf{R}$ is a diagonal matrix, given by $\mathbf{R} = E[\mathbf{V}\mathbf{V}^{\mathrm{T}}]$, and $\mathbf{P}$ is an approximation of the covariance matrix of the errors in the estimated components of $\Delta\mathbf{Y}$

$$\mathbf{P} \cong E[(\Delta\mathbf{Y} - \Delta\hat{\mathbf{Y}})(\Delta\mathbf{Y} - \Delta\hat{\mathbf{Y}})^{\mathrm{T}}]. \tag{12}$$

An alternative and numerically equivalent way of finding the estimative of $\Delta\mathbf{Y}$, given by the Gauss–Markov–Kalman estimator, is to solve the deterministic counterpart optimization problem

$$\text{Minimize } \tfrac{1}{2}\{(\Delta\mathbf{Y} - \Delta\bar{\mathbf{Y}})^{\mathrm{T}}\bar{\mathbf{P}}^{-1}(\Delta\mathbf{Y} - \Delta\bar{\mathbf{Y}}) + (\mathbf{Y} - \mathbf{M}\Delta\mathbf{Y})^{\mathrm{T}}\mathbf{R}^{-1}(\mathbf{Y} - \mathbf{M}\Delta\mathbf{Y})\}. \tag{13}$$

Since constraints satisfaction is necessary for the solution of the problem, the foregoing relation enables the establishment of a weighting relationship between $\bar{\mathbf{P}}$ and $\mathbf{R}$ in order to assure priority to constraint satisfaction over minimizing the objective function.

2.3. Numerical implementation

The numerical implementation of this method is carried out iteratively in a sequence of two phases, namely, (i) phase of constraints acquisition, and (ii) the gradient phase (Rios Neto & Pinto, 1987; Madeira, 1996). The iterative process begins in the phase (i) where from a feasible point a search aims to capture the equality constraints, including the inequality constraints that become active during the search process. When the equality constraints satisfy the limits of tolerable error, a phase (ii) begins to further reduce the objective function value. This process is carried out by relaxing the order of magnitude of error $\mathbf{V}$ (Eq. (10)) to allow priority for a non negligible search step in the direction of the minimum. After completing the gradient phase, phase (i) is repeated in order to reacquire the constraints within the limits of tolerable error. This sequential process continues until the prescribed convergence criterion is met.

The numerical algorithm implemented in this work is based on the procedure proposed by Rios Neto and Pinto (1987) and is summarized below.

(1) The search parameters α and β in each step are given by

$$1 - \alpha = 1 - \beta = s, \tag{14}$$

in which

$$s = \mathrm{Min}\{s_i,\ i = 0,1,2,\ldots,m_h + I_g\}, \tag{15}$$

$$s_0 = 1,$$

$$s_j^2 h_j^2(\bar{\mathbf{Y}}) = 3R_j q_j, \quad j = 1,2,\ldots,m_h,\ q_j \gg 1,$$

$$s_{k+m_h}^2 g_k^2(\bar{\mathbf{Y}}) = 3R_{k+m_h} q_k, \quad k = 1,2,\ldots I_g,\ q_k \gg 1. \tag{16}$$

(2) The dispersion $\boldsymbol{\eta}$ is determined using Eq. (10):

$$\mathbf{Z} = \mathbf{M}(\Delta\bar{\mathbf{Y}} + \boldsymbol{\eta}) + \mathbf{V} = \bar{\mathbf{Z}} + \mathbf{M}\boldsymbol{\eta} \tag{17}$$

and

$$\mathbf{Z} - \bar{\mathbf{Z}} = \boldsymbol{\varepsilon}^Z = \mathbf{M}\boldsymbol{\eta}. \tag{18}$$

Assuming no cross correlation in $\boldsymbol{\varepsilon}^Z$ components, and evaluating their variances by using a maximum likelihood criterion, results:

$$\sum_{j=1}^{n} M_{ij}^2 \bar{P}_{jj} = E[(\varepsilon_i^Z)^2], \quad i = 1,2,\ldots,m_h + I_g. \tag{19}$$

Let

$$E[(\varepsilon_i^Z)^2] = 3R_i q_i. \tag{20}$$

Hence

$$\sum_{j=1}^{n} M_{ij}^2 \bar{P}_{jj} = 3R_i q_i. \tag{21}$$

In the application reported in this paper, the solution of Eq. (21) was found using the following approximation criterion:

$$\bar{P}_{jj} = \mathrm{Max}_i \frac{3R_i q_i}{M_{ij}^2 n_i}, \quad i = 1,2,\ldots,m_h + I_g \text{ and } M_{ij} \neq 0, \tag{22}$$

in which n_i is the number of for each row i of matrix $\mathbf{M}$.

(3) In each step, the search parameter γ was found using the approximation relation:

$$\gamma = \underset{i}{\text{Min}} \frac{\sqrt{3\bar{P}_{ij}}}{\nabla_i F(\bar{\mathbf{Y}})}, \qquad \nabla_i F(\bar{\mathbf{Y}}) \neq 0. \tag{23}$$

3. Launch vehicle open-loop trajectory optimization

3.1. Vehicle modeling and mission description

The *satellite launch vehicle* (VLS) is a conventional nonlifting rocket propelled launch vehicle, composed of four expendable solid-fuel stages. The flights of the first and second stages are assumed to be carried out into the lower atmosphere and the atmosphere effects are neglected for the flight of the third and fourth stages. The burn out time of a given stage coincides with both the current stage structure jettisoning and the ignition of the next stage. A long coasting phase takes place between the third and fourth stage flights.

The mission objective consists of inserting the maximum satellite mass into a circular orbit. The orbit is required to have 750 km of height and an inclination of $-25°$.

In order to assure the vehicle structural integrity, a maximum aerodynamic loading is imposed

$$q\alpha - q\alpha_{\text{MAX}} \leq 0 \tag{24}$$

in which $q\alpha_{\text{MAX}} = 4000$ Pa rad.

3.2. Equations of motion

In the present approach the vehicle is treated as a point mass model, and hence the rotary dynamics are not accounted for. The governing equations are expressed in a moving coordinate system (Madeira, 1996) with the origin at the Earth's center ($r_e = 6\,378\,145$ m) and the x-axis pointing toward the vehicle. The vehicle motion is constrained to the xy-plane, y-axis points forward, and the z-axis is perpendicular to the motion plane, thus completing the right-handed coordinate system.

The equations of motion are then expressed as

$$\dot{X}_1 = \dot{r} = u,$$

$$\dot{X}_2 = \dot{u} = \frac{v^2}{r} - \frac{\mu}{r^2} + \frac{F_T}{M}\sin\alpha_P \cos\alpha_Y - \frac{D_x}{M},$$

$$\dot{X}_3 = \dot{v} = -\frac{uv}{r} + \frac{F_T}{M}\cos\alpha_P \cos\alpha_Y - \frac{D_y}{M},$$

$$\dot{X}_4 = \dot{\psi} = \left(\frac{F_T \sin\alpha_Y - D_Z}{Mv}\right)\frac{\sin\phi}{\sin\theta},$$

$$\dot{X}_5 = \dot{\theta} = \left(\frac{F_T \sin\alpha_Y - D_Z}{Mv}\right)\cos\phi,$$

$$\dot{X}_6 = \dot{\phi} = \frac{v}{r} - \left(\frac{F_T \sin\alpha_Y - D_Z}{Mv}\right),$$

$$\dot{X}_7 = \dot{M} = -\beta, \tag{25}$$

in which

$$F_T = C_V\beta - A_S P_{ATM}(h), \qquad P_{ATM}(h) = \frac{a^2(h)\rho(h)}{\gamma},$$

$$M(t_0) = M_S + M_E + M_P, \qquad Mach = \frac{V}{a},$$

$$\vec{D}(D_x, D_y, D_z), \qquad |\vec{D}| = \tfrac{1}{2}\rho(h)V^2 C_D(Mach, \alpha). \tag{26}$$

In Eq. (25), r, u and v are the vehicle radial distance, the radial and tangential velocities; ψ, θ and ϕ are Euler angles relating the moving coordinate system to a non-rotating Earth-centered inertial system; they are named node angle, inclination angle, and flight path angle, respectively. F_T and D are the vehicle thrust and the aerodynamic drag; α_P and α_Y are the control thrust deflection angles in flight plane (pitch) and out of flight plane (yaw); and μ is the Earth's gravitational constant (3.986012×10^{14} m^3/s^2).

In Eq. (26), C_V and β are the stagewise constant vacuum exhaust gas speed and the propellant mass rate, respectively; A_S is the engine nozzle area, P_{ATM} is the atmospheric pressure, h is the geometric altitude, ρ is the air density, a is the speed of sound, and γ is the gas constant of air ($= 1.40$); M_S, M_E and M_P are payload/satellite mass, the vehicle structure mass, and the propellant mass, respectively; D_x, D_y and D_z are the aerodynamic drag components resolved into the moving coordinate system; V is the total airspeed and α is the angle of attack. The drag coefficient is Mach number and angle of attack dependent and since the problem deals with a nonlifting vehicle the aerodynamic lift is not accounted for into the equation of motion. The geometric altitude dependent functions a and ρ are given by an analytical function (Duffek & Shau, 1975) based on the US Standard Atmosphere (Regan, 1984).

3.3. Statement of the problem

Trajectory optimization problem consists of finding a control history $\mathbf{u}^T(t) = [\alpha_P, \alpha_Y]$, $t_0 \leq t \leq t_f$, that minimizes the objective function

$$F(\mathbf{X}(t_f), t_f) = -X_7(t_f) = -M_S \tag{27}$$

subjected to the final time equality constraints, i.e., the specified circular orbit injection conditions

$$\mathbf{h}(\mathbf{X}(t_f), t_f) = \begin{bmatrix} r(t_f) - r_f \\ u(t_f) \\ v(t_f) - \sqrt{\frac{\mu}{r_f}} \\ \theta(t_f) - \theta_f \end{bmatrix} = \boldsymbol{\varepsilon}, \tag{28}$$

given all the initial state components but X_7, since the vehicle initial mass is not known at all once the satellite mass was not calculated yet; and subjected to the given initial conditions

$$X_7(t_0) = X_{i_0}, \quad i \neq 7, \tag{29}$$

where M_S is the mass at final time, viz., the payload mass to be injected into orbit, and the aerodynamic loading inequality constraint is converted into an equality constraint. Let X_8 be an additional state variable, such that

$$X_8 = \begin{cases} q\alpha - q\alpha_{MAX} & \text{if } q\alpha - q\alpha_{MAX} \geq 0, \\ 0 & \text{if } q\alpha - q\alpha_{MAX} < 0, \end{cases}$$

in which $X_8(t_0) = 0$, and let h_5 be an additional equality constraint, such that

$$h_5(\mathbf{X}(t_f), t_f) = X_8(t_f) = \varepsilon_5. \tag{30}$$

Hence, the additional equality constraint, to be met at the final time, assures the inequality constraint will not be violated along the whole vehicle flight trajectory.

3.4. Parametrization of control history

In order to parametrize the control history, the trajectory is first divided into a sequence of segments, separated from each other by meshpoints. Every discontinuity in state and control coincides with a meshpoint. Thus, for each burning out time a meshpoint is assigned due to the stage structure jettisoning.

Using a Rayleigh–Ritz method, the control history can be approximated by an arbitrarily parametrized function (Williamson, 1971)

$$\mathbf{u}(t) \cong \mathbf{u}(\mathbf{a}, t). \tag{31}$$

Once the values of the parameter vector $\mathbf{a}$ are determined, $\mathbf{u}(\mathbf{a}, t)$ depends only on time. Therefore, the control in each flight trajectory segment is approximated as arcs of a function that is usually taken to be a polynomial (e.g. Williamson, 1971; Rios Neto & Ceballos, 1979; Ceballos & Rios Neto, 1981; Ceballos, 1979). In this paper, $\mathbf{u}(\mathbf{a}, t)$ is approximated by linear functions, so that the control history is determined by the parameters:

$$\mathbf{a}_P^T = [a_{P_0}, a_{P_1}, \ldots, a_{P_N}], \qquad \mathbf{a}_Y^T = [a_{Y_0}, a_{Y_1}, \ldots, a_{Y_N}],$$

where a_{P_i} and a_{Y_i} are the pitch and yaw control values at the ith meshpoint, and N is the number of flight trajectory segments. The control for the ith trajectory segment is then given by

$$\alpha_P(t) = (a_{P_{i+1}} - a_{P_i}) \frac{t - t_i}{t_{i+1} - t_i} + a_{P_i},$$

$$\alpha_Y(t) = (a_{Y_{i+1}} - a_{Y_i}) \frac{t - t_i}{t_{i+1} - t_i} + a_{Y_i}, \tag{32}$$

in which $t_i \leq t \leq t_{i+1}$ and $t_0 < t_1 < \cdots < t_N \equiv t_f$.

3.5. Problem solution

The equations of motion depend only on the parameter vectors $\mathbf{a}_P$ and $\mathbf{a}_Y$, the duration of coasting flight t_C, and on the satellite mass M_S. The trajectory optimization solution problem consists of determining an optimizable parameter array $\mathbf{y}$, given by

$$\mathbf{y}^T = [\mathbf{a}_P^T, \mathbf{a}_Y^T, t_C, M_S] \tag{33}$$

that

$$\text{Minimizes} \quad F(\mathbf{y}) \tag{34}$$

$$\text{subject to} \quad \mathbf{h}(\mathbf{y}) = \boldsymbol{\varepsilon}, \tag{35}$$

where F and $\mathbf{h}$ have already been defined in Eqs. (27), (28) and (30).

The Jacobian matrix

$$\left[\frac{d\mathbf{h}}{d\mathbf{y}}\right]_{t=t_f}$$

needed in the linearized approximation (see Eq. (6)) is given by

$$\left[\frac{d\mathbf{h}}{d\mathbf{y}}\right]_{t=t_f} = \left[\frac{\partial \mathbf{h}}{\partial \mathbf{X}}\right]_{t=t_f} \left[\frac{\partial \mathbf{X}}{\partial \mathbf{y}}\right]_{t=t_f} + \frac{\partial \mathbf{h}}{\partial \mathbf{y}}. \tag{36}$$

Since the constraint vector $\mathbf{h}$ does not depend explicitly upon the optimizable parameter array $\mathbf{y}$, the Jacobian $\partial \mathbf{h}/\partial \mathbf{y}$ is a null matrix. Unlike

$$\left[\frac{\partial \mathbf{h}}{\partial \mathbf{X}}\right]_{t=t_f},$$

which has a straightforward analytical form, the Jacobian

$$\left[\frac{\partial \mathbf{X}}{\partial \mathbf{y}}\right]_{t=t_f}$$

is calculated numerically using the central-difference method (Gill, Murray & Wright, 1981).

3.6. Open-loop trajectory optimization simulations

In what follows, results obtained for a typical MEC-B (Brazilian Complete Space Mission) satellite mission, from the Alcântara launch site, using a solid propelled four stages launching vehicle, to place a satellite into a 750 km height circular orbit of $-25°$ of inclination are presented (Madeira, 1996).

With the aim of maximizing the satellite mass capability, three different strategies have been implemented. In the first strategy, a minimum number of parameters have been used. The pitch and yaw steering controls vary linearly from the current stage ignition till the burn out time/stage structure jettison. After that, the controls switch to another slope and so on. The second strategy is similar to the first one, except that it assigns two straight line segments for the control vector components in each flight stage; and the third, most refined strategy, assigns four straight-line segments for the control vector components in each flight stage.

Even though the first strategy is the least refined one, the results obtained and depicted in Fig. 1 and Table 1 indicate it yields quite satisfactory results when compared to an optimal multiple shooting solution to the same problem (Zerlotti, 1990). Moreover, the second and third strategies add no further improvements on the results compared to the first strategy. The height profiles for the second and third strategies were not shown in Fig. 1 since they are quite so close to the first one that they overlap for almost the entire flight path. For the three implemented near-optimal strategies, the control profiles as well as state profiles are closely related to their optimal counterpart (Madeira, 1996). However, the profiles of the aerodynamic states α (angle of attack) and $q\alpha$ exhibit major differences compared to the optimal counterparts. Such differences are due to the fact that at the meshpoint times the control switches from one slope to another (Madeira, 1996).

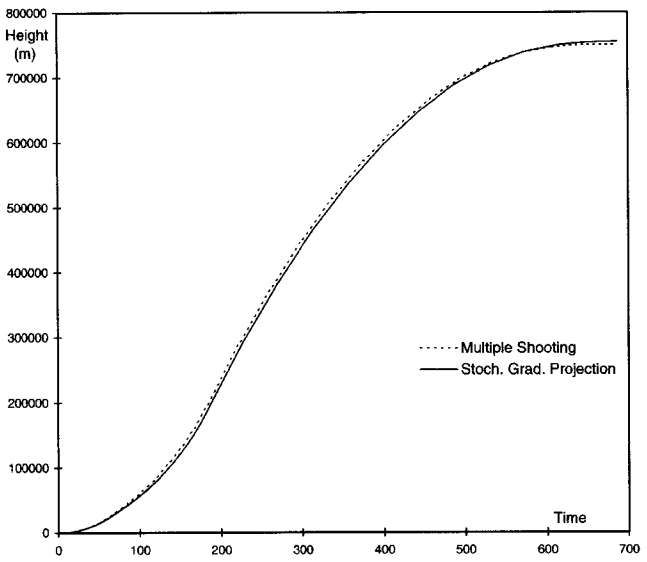

Fig. 1. Open-loop solution height vs. time.

4. Launch vehicle closed-loop guidance and control procedure

The solution of a trajectory optimization problem gives a parameter array $\mathbf{y}$ (Eq. (33)). Under ideal flight conditions, i.e., a flight in which the effects of model uncertainties and environmental perturbations are negligible, the use of $\mathbf{y}$ throughout the flight trajectory in an open-loop fashion will lead to the satisfaction of the condition:

$$h_j(\mathbf{y}) \leq |\varepsilon_j|, \tag{37}$$

that is, each mission constraint h_j will be satisfied with as much accuracy ε_j as our trajectory optimization procedure performance allows.

However, for a real flight that is no longer true. Since most of the parameters required for computing $\mathbf{y}$ are subjected to uncertainties, and the environmental effects tend to perturbate the vehicle's flight away from the optimal nominal trajectory, an onboard in-flight updating of parameter array $\mathbf{y}$ is in order, otherwise unsuccessful constraints satisfaction will result, leading to the mission objectives fulfillment failure. Such an onboard in-flight updating demands for a closed-loop guidance and control procedure.

Since now one is concerned with an actual flight mission, the vehicle initial mass is a known parameter and hence the satellite mass too. The closed-loop guidance and control problem does not account for the satellite mass optimization. Hence, this problem does not require the minimization of an objective function and the

Table 1
Open-loop solution: constraints satisfaction and the resulting satellite mass

		h_1 (m)	h_2 (m/s)	h_3 (m/s)	h_4 (deg)	h_5 (Pa s)	M_S (kg)
Stochastic	1st strategy	−5.0582E−3	−7.0608E−6	−4.1137E−6	−2.7217E−8	1.6739E−7	182.9730
Gradient	2nd strategy	−6.6903E−3	−2.4927E−5	−2.2198E−5	1.8844E−8	4.5541E−8	186.1121
Projection	3rd strategy	−4.4446E−5	−7.1028E−8	−1.4814E−8	5.4622E−12	3.1555E−9	185.7202
Multiple shooting[26]		±5.E−3	±5.E−3	±5.E−3	—	—	187.8955

left-hand side of Eq. (8) is set equal to zero, leading to the following a priori information:

$$\mathbf{y}^{\text{old}} = \mathbf{y}^{\text{new}} + \boldsymbol{\eta}, \tag{38}$$

where $\mathbf{y}^{\text{old}}$ is the previously known part of the vector of parameters, needed to be updated for the remaining part of the flight control, and it is assumed that the vehicle deviation takes place inside a suitable neighborhood of the reference trajectory such that the new control history $\mathbf{y}^{\text{new}}$ lies inside a region around the old control history $\mathbf{y}^{\text{old}}$, bounded by the uniformly distributed unbiased stochastic error vector $\boldsymbol{\eta}$. For the closed-loop guidance and control problem the observation like equation for constraint satisfaction is the same as Eq. (35) of the trajectory optimization problem. However, for the sake of real time operation feasibility, each control history updating will be performed in a single iteration, implying α equal to zero in Eq. (6).

The closed-loop guidance and control then consists of updating the part left of control history $\mathbf{y}^{\text{T}} = [\mathbf{a}_P^{\text{T}}, \mathbf{a}_Y^{\text{T}}, t_{\text{C}}]$ at some prescribed time instants during the flight, solving the filtering problem:

$$\mathbf{y}^{\text{old}} = \mathbf{y}^{\text{new}} + \boldsymbol{\eta}, \qquad \mathbf{h}(\mathbf{y}^{\text{new}}) = \boldsymbol{\varepsilon}. \tag{39}$$

After linear perturbation this problem is converted into a linear optimal filtering problem solved with the Gauss–Markov–Kalman estimator (Eq. (11)) providing the optimum correction increment $\Delta\hat{\mathbf{y}}$, leading to

$$\hat{\mathbf{y}}^{\text{new}} = \mathbf{y}^{\text{old}} + \Delta\hat{\mathbf{y}}. \tag{40}$$

For the onboard in-flight control, the actual state $\mathbf{X}(\tau_k)$ at some assigned meshpoint time τ_k ($k = 1, 2, \ldots, L$, $\tau_0 \equiv t_0, \tau_{\text{f}} \equiv t_{\text{f}}$) is not, to a lesser extent, equal to the nominal reference state $\mathbf{X}^*(\tau_k)$. The nominal reference state was found earlier, by the off-line trajectory optimization procedure and afterwards by the most recent update pf the closed-loop guidance and control. The actual state is externally supplied by some navigation sensor output, e.g., GPS, INS, a combination GPS/INS, etc. The stochastic gradient projection method takes the information provided by the actual state $\mathbf{X}(\tau_k)$ as start-point to update the control history which will actually be used in the time interval (τ_k, τ_{k+1}). The time meshpoints assignment follows the same guidelines stated for parametrization of control history.

At beginning of the flight (τ_0), the actual control history to be used until τ_1 is

$$\mathbf{y}^0 = [\mathbf{a}_0^0, \mathbf{a}_1^0, \ldots, \mathbf{a}_N^0, t_{\text{C}}^0]^{\text{T}} \tag{41}$$

which has been previously computed in the open loop solution.

In order to simulate the real flight conditions, dynamic model parameter uncertainties are artificially introduced and Eq. (38) are numerically integrated. The perturbed value of a parameter p_j due to model typical uncertainties Δp_j is defined as:

$$\bar{p}_j = p_j + rand_j \Delta p_j, \tag{42}$$

in which

$$-1 \le rand_j \le 1 \tag{43}$$

is an unbiased uniformly distributed random number.

It must be stressed that the calculation for updating the control history $\mathbf{y}$ are performed using the unperturbed parameters p_j. The perturbed parameters $\bar{p}_j$ are used ad hoc to drift the vehicle away from the nominal reference trajectory through the introduction of model uncertainties in an attempt to simulate a real flight. Therefore, in order to accomplish the filtering task, the perturbed values are not known a priori, only their effects are observed a posteriori.

Prior to the kth updating, the actual control history is

$$\mathbf{y}^{k-1} = [\mathbf{a}_j^{k-1}, \mathbf{a}_{j+1}^{k-1}, \ldots, \mathbf{a}_N^{k-1}, t_{\text{C}}^{k-1}]^{\text{T}}, \quad \tau_{k-1} < t < \tau_k, \tag{44a}$$

in which $t_j < \tau_{k-1} < t_{j+1}$. The actual state $\mathbf{X}^{k-1}(\tau_k)$ is found by taking the perturbed parameters $\bar{p}_j$ and the actual control history $\mathbf{y}^{k-1}$ into the dynamic Eq. (38) and integrating them from τ_{k-1} to τ_k and taking $\mathbf{X}^{k-1}(\tau_{k-1})$ as initial condition.

If $\tau_k < t_{j+1}$, then $\mathbf{a}_j^{k-1}$ is still the first actual vector component of $\mathbf{y}$. Thus,

$$\mathbf{a}_j^{k-1}(\tau_k) = (\mathbf{a}_{j+1}^{k-1} - \mathbf{a}_j^{k-1}(\tau_{k-1}))\frac{\tau_k - t_j}{t_{j+1} - t_j} + \mathbf{a}_j^{k-1}(\tau_{k-1}) \tag{45a}$$

and $\mathbf{a}_j^{k-1}(\tau_k)$ replaces $\mathbf{a}_j^{k-1}(\tau_{k-1})$ into Eq. (44a).

If, $\tau_k > t_{j+1}$, then $\mathbf{a}_j$ may be dropped from the control history, leading to

$$\mathbf{y}^{k-1} = [\mathbf{a}_{j+1}^{k-1}, \mathbf{a}_{j+2}^{k-1}, \ldots, \mathbf{a}_N^{k-1}, t_{\text{C}}^{k-1}]^{\text{T}} \tag{44b}$$

and thus

$$\mathbf{a}_{j+1}^{k-1}(\tau_k) = (\mathbf{a}_{j+2}^{k-1} - \mathbf{a}_{j+1}^{k-1}(\tau_{k-1}))\frac{\tau_k - t_{j+1}}{t_{j+2} - t_{j+1}} + \mathbf{a}_{j+1}^{k-1}(\tau_{k-1}) \tag{45b}$$

replaces $\mathbf{a}_{j+1}^{k-1}(\tau_{k-1})$ into Eq. (44b).

Once the first actual vector component has been suitably updated for $t = \tau_k$ (Eq. (45)), the control history $\mathbf{y}^{k-1}$ (Eq. (44)) is taken to be the a priori information $\mathbf{y}^{\text{odd}}$ (Eq. (39)) and, from an initial state $\mathbf{X}^{k-1}(\tau_k)$, the updated control history $\hat{\mathbf{y}}^{\text{new}} = \mathbf{y}^k$ is next calculated using the stochastic gradient projection method. The new control history $\mathbf{y}^k$ will be the actual control history to be used in the time interval $\tau_k < t < \tau_{k+1}$.

4.1. Closed-loop solution simulation

The numerical simulations of the closed-loop guidance and control procedure were performed using typical parameter uncertainties for the MEC-B launch vehicle (Madeira, 1996), as depicted in Table 2.

The control history updating was performed three times during each booster phase and once during the coasting phase ($L = 13$, number of meshpoints τ_k). This approach leads approximately to one updating at every 20 s during the booster phases. Such a low updating frequency is part of an endeavor to achieve real time operation feasibility.

The real time operation will not be addressed. For the purposes of this phase of exploratory study it is assumed that closed-loop guidance and control procedure consists of a reactive system operating under the hypothesis of synchronous approach (Benveniste & Berry, 1991).

The synchronous approach hypothesis considers an idealized system which produces its output synchronously with its input. Therefore, at time τ_k, when the kth updating takes place, the actual state $\mathbf{X}(\tau_k)$ (input) is determined and hence the new control history $\mathbf{y}^k$ (output) is synchronously found, then replacing at the same time the old control history $\mathbf{y}^{k-1}$. In other words, it is assumed that the elapsed time for computing $\mathbf{y}^k$ is negligible and at $t = \tau_k$ the actual control history switches from $\mathbf{y}^{k-1}$ to $\mathbf{y}^k$.

In this paper the numerical results for two case studies are presented. The first case study considers the standard MEC-B launch vehicle configuration. The second case study considers the upper stage burning time as being free.

4.1.1. Case study 1: the standard case

The standard case considers the same launch vehicle configuration used for open-loop trajectory optimization and all assumptions done up to this point remains still applicable. Two realizations, named A and B, found in tests (Madeira, 1996) to be representative of the range of behavior due to typical perturbations were selected for presentation.

The Fig. 2 illustrates the differences in the pitch and yaw control histories for realizations A and B, respectively, as compared to the open-loop control histories found by the trajectory optimization procedure. Though the entire left control history is calculated for every updating, only the control history actually used is shown. During the coasting phase, between the third and fourth stage flights, there is no control action and therefore no control history is shown. Table 3 shows the resulting orbit characteristics.

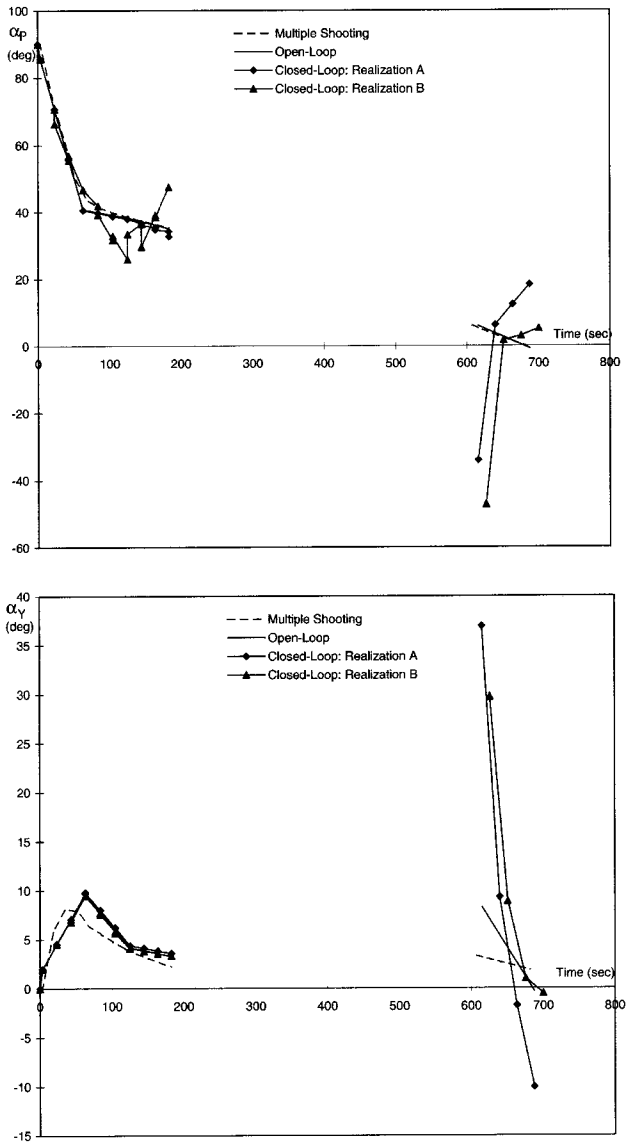

Fig. 2. Control vs. time for the standard case (case study 1).

Table 2
Parameter uncertainties

Parameter	Uncertainty (%)	Parameter	Uncertainty (%)
C_{D0}	10	C_V	5
C_{Lz}	10	β	0.5
M_E	1	a	0.1
M_P	1.5	γ	1
ρ	10		

Table 3
Orbit characteristics for the closed loop standard case (case study 1)

	Realization	Apogee height (m)	Orbit eccentricity	Orbit inclination (deg)
A	Closed-loop	750051.3786	7.0763E − 6	− 25.000159
	Open-loop	955135.2059	2.5867E − 2	− 25.312379
B	Closed-loop	731829.9049	2.5564E − 3	− 24.999736
	Open-loop	687526.6107	1.3953E − 2	− 24.952062
	Nominal orbit	750000	0	− 25

The discontinuities in the closed-loop control histories (Fig. 2) are due to the switching from one control history to the next, at the updating times. Moreover, the upper stage flight demands larger variations on the closed-loop control histories once the time-to-go is even more close to zero and the upper stage burning time is fixed.

4.1.2. Case study 2: free upper stage burning time

The MEC-B launch vehicle is composed by four stages propelled by solid-fuel rocket engines. Solid-fuel rocket engines have two features which distinguish them from their liquid-fuel counterparts, namely, nonthrottleability and nonshutoff capability (burning time fixed). For closed-loop guidance and control purposes, the solid-fuel features become a drawback. In order to cope with the uncertainties and perturbations, the additional control degree of freedom assured by the throttleability and shutoff capability of a liquid-fuel propelled rocket engine would improve the resulting orbit characteristics. Therefore, a liquid rocket engine would be desirable at least for upper stages propulsion.

In order to investigate the performance of a liquid-fuel propelled upper stage during a real flight mission, the time of burning of the fourth stage was left to be free, i.e., it was assumed that the fourth stage exhibits the shutoff capability. This approach is equivalent to assume that the fourth stage is propelled by a liquid-fuel rocket engine at full-throttle, displaying the same characteristics of its solid-fuel counterpart, except the burning time which, due to the shutoff capability, is free.

Initially, a nominal reference time of burning for the fourth stage equal to the original fourth stage solid-fuel time of burning was assumed. Such a time was then appended to the control history $\mathbf{y}$ and was hence updated accordingly. Also, even the resulting mass of the fourth stage propellant and satellite was known, it was assumed that their masses are a priori unknown apart.

Note that a fraction of the satellite mass calculated by the trajectory optimization problem should be allocated to an additional propellant mass, leading to a smaller actual satellite mass. With this approach after performing some simulations, one should be able to establish an additional propellant mass which could safely accomplish the mission. On the other hand, one could explore the other liquid-fuel rocket feature by assuming one can control the mass flow rate (throttleability). However, the implementation of such a feature is not so straightforward.

Fig. 3 presents the closed-loop control histories behavior obtained in the simulation study for realizations A and B as compared to the open-loop control history. It can be noticed that the additional degree of freedom provided by the shutoff capability turned out to demand smaller variations on the closed-loop control histories for the upper stage flight as compared to the standard case. Table 4 shows the resulting orbit characteristics and the fourth stage time of burning.

4.2. Closed-loop results analysis

For the standard case, the results presented show that for a real flight, the closed-loop guidance and control procedure yields smaller orbital injection errors. For the MEC-B data collection class satellite, the tolerable errors for orbital injection are (Madeira, 1996):

- apogee height: $\pm$ 50 km,
- orbit eccentricity: $\pm$ 0.05,
- orbit inclination: °.

Accordingly to Table 3, for all realizations the closed-loop procedure could inject successfully the satellite into the desired orbit; the orbital injection errors are inside the tolerable interval. However, the application of the control history in an open-loop fashion could not achieve the apogee height error inside the tolerable interval.

For the free upper stage burning time, the results presented suggest that a liquid-fuel propelled rocket engine for the upper stage propulsion would achieve smaller orbit injection errors. Beyond, an upper stage configuration with a burning time additional capability of about 2 s seems to be suitable for complete the mission safely. Such a configuration demands approximately for

a satellite mass fraction in excess of 23 kg to be allocated as additional propellant mass. The amount of fuel which could eventually be saved may be further used for execution of orbital maneuvers in order to improve the satellite lifetime.

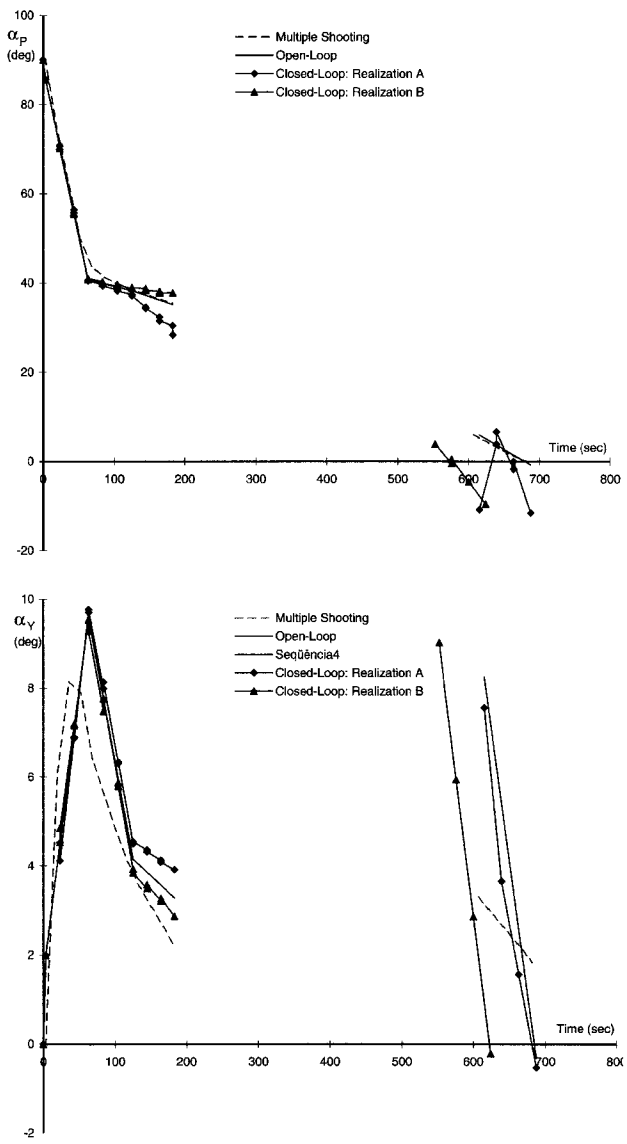

Fig. 3. Control vs. time for the free upper stage burning time (case study 2).

5. Conclusions

The use of a stochastic gradient projection method for trajectory optimization and low frequency closed-loop satellite launch vehicle guidance and control was presented and tested.

The trajectory optimization results obtained show the potential of the stochastic gradient projection method for accurate orbital injection of payloads. Even the poorest approach for the control history parametrization (the first strategy) achieved tight constraints satisfaction. The method was also successful in maximizing the payload capability. The satellite mass obtained using the second strategy was only 0.95% below the solution reported by Zerlotti (1990) who used an optimal indirect multiple shooting method.

The proposed closed-loop guidance and control procedure was able to cope with the uncertainties and perturbations typically found during a real flight mission and inject satisfactorily a data collection class satellite into orbit. The computational workload demanded and reliability indicate the feasibility of real-time application.

Acknowledgements

This research was supported by CNPq — National Research Council. It was developed while the first author was graduate student at the Technological Institute of Aeronautics (ITA) and the second author was senior researcher at the National Space Research Institute (INPE).

References

Benveniste, A., & Berry, G. (1991). The synchronous approach to reactive and real-time systems. *Proceedings of the IEEE, 70*, 1270–1282.

Betts, J. T. (1994). Optimal interplanetary orbit transfer by direct transcription. *The Journal of Astronautical Sciences, 42*, 247–268.

Betts, J. T., & Huffman, W. P. (1991). Trajectory optimization on a parallel processor. *Journal of Guidance, Control, and Dynamics, 14*, 431–439.

Breakwell, J. V. (1959). The optimization of trajectories. *Journal SIAM, 7*, 215–247.

Table 4
Orbit characteristics for the closed loop and free upper stage burning time

Realization	Apogee height (m)	Orbit eccentricity	Orbit inclination (deg)	4th stage burning time (s)
A	757450.8277	1.1301E − 3	− 25.001406	70.100870
B	746865.1286	4.4664E − 4	− 24.998467	73.157844
Nominal orbit	750000	0	− 25	72

Burlirsch, R., & Chudej, K. (1992). Guidance and trajectory optimization under state constraints applied to a sänger-type vehicle. *12th IFAC symposium*, Ottobrunn (pp. 483–488).

Ceballos, D. C. (1979). *Aproximações Sub-Ótimas para o Controle em Programas Dinâmicos de Otimização*. M.Sc. thesis, National Space Research Institute (INPE), São José dos Campos, Brazil.

Ceballos, D. C., & Rios Neto, A. (1981). Linear programming and suboptimal solutions of dynamical systems control problems. *International symposium on spacecraft flight dynamics*, ESA SP-160, Darmstadt, Germany (pp. 239–243). (ISSN - 039-6566).

Corban, J. E., Calise, A. J., & Flandro, G. A. (1991). Rapid near-optimal aerospace plane trajectory generation and guidance. *Journal of Guidance, Control, and Dynamics*, *14*, 1181–1190.

Coverstone-Carroll, V., & Williams, S. N. (1994). Optimal low thrust trajectories using differential inclusion concepts. *The Journal of Astronautical Sciences*, *42*, 379–393.

Duffek, W., & Shau, G. C. (1975). Optimierung der Aufstiegsbahn eines 4stufigen Trägers für Synchronbahn-Missionen. DLR, Forschungsbericht 75-04, Oberpfaffenhofen.

Enright, P. J., & Conway, B. A. (1992). Discrete approximations to optimal trajectories using direct transcription and nonlinear programming. *Journal of Guidance, Control, and Dynamics*, *4*, 994–1002.

Feeley, T. S., & Speyer, J. L. (1994). Techniques for developing approximate optimal advanced launch system guidance. *Journal of Guidance, Control, and Dynamics*, *17*, 889–896.

Gill, P. E., Murray, W., & Wright, M. H. (1981). *Practical optimization*. London: Academic Press.

Hargraves, C. R., & Paris, S. W. (1987). Direct trajectory optimization using nonlinear programming and collocation. *Journal of Guidance, Control, and Dynamics*, *10*, 338–342.

Hodges, D. H., Calise, A. J., Bless, R. R., & Leung, M. (1992). Finite element method for optimal guidance of an advanced launch vehicle. *Journal of Guidance, Control, and Dynamics*, *15*, 664–671.

Jazwinski, A. H. (1970). *Stochastic process and filtering theory*. New York: Academic Press.

Leung, M. S. K., & Calise, A. J. (1994). Hybrid approach to near-optimal vehicle guidance. *Journal of Guidance, Control, and Dynamics*, *17*, 881–888.

Lu, P. (1993). Inverse dynamics approach to trajectory optimization for an aerospace plane. *Journal of Guidance, Control, and Dynamics*, *16*, 726–732.

Madeira, F. (1996). *Guiagem e Controle Não-Linear Sub-Ótimo de Veículos Lançadores de Satélites em Malha Fechada e em Tempo Quase Real*. Ph.D. thesis, Dept. of Aeronautical Engineering, Technological Institute of Aeronautics (ITA), São José dos Campos, Brazil.

Mease, K. D., & van Buren, M. A. (1994). Geometric synthesis of aerospace plane ascent guidance logic. *Automatica*, *30*, 1839–1849.

Prado, A. F. B. A., & Rios Neto, A. (1994). A stochastic approach to the problem of spacecraft optimal maneuveurs. *Revista Brasileira de Ciências Mecânicas*, *XVI*, 268–278.

Psiaki, M. L., & Park, K. H. (1992). Parallel solver for trajectory optimization search directions. *Journal of Optimization Theory and Applications*, *73*, 519–546.

Regan, F. J. (1984). *Re-entry vehicle dynamics*. AIAA Education Series (pp. 5–22). New York: AIAA.

Richard, F., & Christophe, B. (1995). Open and closed loop guidance for an airbreathing winged launch vehicle. *Acta Astronautica*, *35*, 83–97.

Rios Neto, A., & Ceballos, D. C. (1979). Approximation by polynomial arcs to generate suboptimal numerical solutions in control problems. *V Congresso Brasileiro de Engenharia Mecânica*, Campinas, Brazil, vol. C (pp. 34–43).

Rios Neto, A., & Madeira, F. (1997). Stochastic gradient projection method applied to an earth mars orbit transfer problem. *14th Brazilian congress of mechanical engineering*, Bauru, Paper Number 211, Brazil.

Rios Neto, A., & Pinto, R. L. U. F. (1987). A stochastic approach to generate a projection of the gradient type method. VIII *Congresso Latino-Americano e Ibérico Sobre Métodos Computacionais para Engenharia*, Rio de Janeiro, Brazil (pp. 331–345).

Sachs, G., Drexler, J., & Stich, R. (1991). Optimal control of ascent trajectories and rotary dynamics for wingless orbital stages. *Acta Astronautica*, *25*, 463–471.

Seywald, H. (1993). Trajectory optimization based on differential inclusion. NASA CR-4501.

da Silva, P. S. (1994). *O Método das Correções Repetitivas para Guiagem Ótima de Veículos Lançadores de Satélites*. M.Sc. thesis, Dept. of Electronical Engineering, Technological Institute of Aeronautics, São José dos Campos, Brazil.

Sinha, S. K., Shrivastava, S. K., Bhat, M. S., & Prabhu, K. S. (1989). Optimal explicit guidance for three-dimensional launch trajectory. *Acta Astronautica*, *19*, 115–123.

Smania, A. C. M., & Rios Neto, A. (1988). Otimização de Trajetórias de Veículos Lançadores de Satélite. *SBA: Controle & Automação*, *2*, 121–125.

Tang, S., & Conway, B. A. (1995). Optimization of low-thrust interplanetary trajectories using collocation and nonlinear programming. *Journal of Guidance, Control, and Dynamics*, *18*, 599–604.

Vittal, R. V., & Bhat, M. S. (1991). An explicit closed-loop guidance for launch vehicles. *Acta Astronautica*, *25*, 119–129.

Williamson, W. E. (1971). Use of polynomial approximations to calculate suboptimal controls. *AIAA Journal*, *9*, 2271–2273.

Wirthman, D., Park, S. Y., & Vadali, S. R. (1995). Trajectory optimization using parallel shooting method on parallel computer. *Journal of Guidance, Control, and Dynamics*, *18*, 377–379.

Zerlotti, R.F. (1990). *Otimização da Trajetória Ascendente de Veículos Lançadores de Satélites Usando o Algoritmo dos Múltiplos Tiros*. M.Sc. Thesis, Dept. of Aeronautical Engineering, Technological Institute of Aeronautics, São José dos Campos, Brazil.

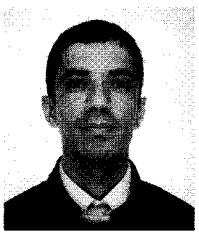

Fernando Madeira was born in Brazil in 1966. He received his B.S. degree in Physics from Federal University of Santa Catarina — UFSC in 1987, his M.S. degree in Physics from State University of Campinas — UNICAMP in 1990, and his Ph.D. degree in Aeronautical Engineering from Technological Institute of Aeronautics — ITA in 1996. Since 1996 he has been with the Flight Mechanics Group at EMBRAER, where he has worked on the development of regional jets ERJ-145, ERJ-135, and ERJ-170, and on the light attack airplane EMB-314/ALX. He is member of the Brazilian Society of Automatica — SBA and Brazilian Society of Mechanical Sciences — ABCM.

Atair Rios Neto was born in Brazil on October 31, 1942. He Received his B.S. degree in Mechanical Engineering from the University of São Paulo — USP in 1966 and a Ph.D. degree from the University of Texas at Austin in 1973.

From 1967 to 1979 he held the position of Professor at the Polytechnic School of Engineering of the University of São Paulo developing teaching and research activities in applied mechanics and optimal control. During this period while attending his doctoral program he was a Research Assistant at the Department of Aerospace Engineering of the University of Texas at Austin (1969 to 1971). Still during this period he helped to organize: the first graduate course in the area of systems control of the University of São Paulo (1973–1974); the first Orbital Dynamics and Control group of Brazil, at

the National Space Research Institute — INPE (1976–1978); and the School of Engineering of Ilha Solteira of the Paulista State University — UNESP (1979). From 1980 to 1996 he held the position of researcher at the National Space Research Institute — INPE, developing research and graduate teaching activities in space mechanics and control. During this period he organized, and was the first head of, the Space Mechanics and Control Department of INPE (1982–1985); the president of the Brazilian Society of Automatica (1985–1987); the general manager of the corporate university of *Empresa brasileira de Aeronáutica* — EMBRAER (on leave, 1988–1991); the head of the Center of Special Technologies of INPE (1995–1996). Since 1997, he is a full professor and researcher at the University of the Paraiba Valley — UNIVAP, in the Institute of Research and Development — IPD, as the coordinator of the Neural Networks in Signal Processing and Optimal Control of Dynamic Systems research group.

His scientific and technical publications have been mainly in the areas of statellite launching, attitude and orbit control and applied optimal control. His current research interest is on neural networks applied to control.

Dr. Rios Neto is a Sigma Gamma Tau member; a cofounder member of the Brazilian Society of Automatica — SBA (affiliated to IFAC); a cofounder member of the Brazilian Society of Mechanical Sciences — ABCM. He has served on many national and international committees, has been for many years an *Ad Hoc* consultant for Brazilian research agencies; and presently is also a member of the editorial board of the Journal of the Brazilian Society of Mechanical Sciences.